MAO A AND B RADIOTRACERS SHOW A REDUCED ARTERIAL PLASMA INPUT FUNCTION, PROLONGED LUNG RETENTION AND REDUCED MAO IN SMOKERS vs NON-SMOKERS

J. Logan, J.S. Fowler.
Chemistry, Brookhaven National Laboratory, Upton, NY, United States.

We have previously shown that smokers have reduced human brain monoamine oxidase A and B (MAO A and B) using PET and the irreversible mechanism-based radiotracers [^{11}C]clorgyline and [^{11}C]deprenyl (CLG and DEP) and their deuterium-substituted derivatives (D CLG, D DEP) (Fowler er al., 1996). We also compared MAO in peripheral organs in non-smokers and smokers using the deuterium isotope effect to assess specificity for MAO. In applying a three-compartment model to time–activity data for the lung, we found that smokers had reduced k3, the model term proportional to MAO activity, even though the lung uptake at plateau was similar for the two groups. To investigate the factors contributing to a reduced value of k3 even when the plateau phase of the time-activity curves were similar, we re-examined the radiotracer kinetics and the robustness of the model term k3 for estimating lung MAO A and B. Methods: Time-activity data from lung and arterial plasma over a 60 min study time were used from 7 non-smokers and 7 smokers scanned with CLG and D CLG and 5 non-smokers and 9 smokers scanned previously with DEP and D DEP (Fowler et al., 2003). The integrals for the arterial plasma time-activity curves were compared at an early time point (2.5 min) and at the end of the study (55 min). A three-compartment irreversible model was used to estimate differences between smokers and nonsmokers for K1 (plasma to lung transfer term) and the stability of the model term k3 while varying model assumptions for the relative fractions of lung tissue, blood and air in the PET voxel. Results: The peak in the arterial plasma input function and the integral of the arterial plasma time-activity curve over the first 2.5 min after radiotracer injection was significantly lower for smokers for both CLG and D CLG and DEP and D DEP. Peak and plateau C-11 concentration in the lung was similar for the two groups. However, the decline from peak to plateau for the lungs (occurring ~2-20 minutes post injection) was slower for smokers. K1 was larger in smokers, while k3 was found to be significantly lower in smokers ($p<0.0005$) indicating a 50% reduction in MAO A for both CLG and D CLG. For DEP, k3 was also significantly lower in smokers ($p<0.0005$) giving a reduction of ~80% in lung MAO B although there was a very large coefficient of variation in the smoker's k3. Values of λ (K1/k2) were also larger for smokers consistent with a longer lung retention of the non-MAO-bound tracer which is consistent with the slower decline in uptake from peak to plateau for smokers for the lungs. The values of k3 are insensitive to model assumptions of variations in air and tissue fraction in the PET voxel. Conclusions: Model estimates of k3, which indicate that smokers have lower lung MAO A and B activity than nonsmokers, are robust and are insensitive to variations in model assumptions for relative fractions of lung tissue, blood and air in the PET voxel. The values of k3 are largely governed by the slower clearance of non-MAO-bound radioactivity from the lung. This may reflect tobacco-smoke-induced inflammatory processes and cell injury. This study also revealed that the concentration of the MAO A and B radiotracers in the arterial plasma at short times after radiotracer injection is significantly lower for smokers which may be due to retention by the smoker's lungs. If this is generally true for other substances which are administered intravenously, then this needs to be considered as a variable which may contribute to different short term behavioral and therapeutic responses to intravenously administered compounds for non-smokers vs smokers. Supported by DOE-OBER and NIH.

Keywords: Lung and Plasma Kinetics, Monoamine Oxidase, Smoker vs Non-Smoker

COMPARISON OF HIGH RESOLUTION MOUSE PET/CT IMAGING AND CONVENTIONAL BIODISTRIBUTIONS OF COPPER-64-LABELLED ANTIBODIES

M.R. Lewis,[1] J.N. Bryan,[1] F. Jia,[1] H. Mohsin,[2] G. Sivaguru,[1] W.H. Miller,[3] C.J. Henry,[1] C.J. Anderson.[4]

[1]Veterinary Medicine and Surgery, University of Missouri; [2]Chemistry; [3]Nuclear Science and Engineering, University of Missouri, Columbia, MO, United States; [4]Mallinckrodt Institute of Radiology, Washington University, St. Louis, MO, United States.

Internalizing ^{64}Cu-labelled monoclonal antibodies (mAbs) have shown remarkable efficacy for radioimmunotherapy (RIT) in rodent models, at far lower absorbed radiation doses than generally considered tumoricidal (1). We developed a two-antibody model of ^{64}Cu RIT, consisting of internalizing and non-internalizing mAbs with high tumor uptakes in LS174T-bearing nude mice (2). The present studies used this model to compare tumor biodistributions and dosimetry, obtained by high resolution PET/CT imaging and conventional methods.

Mice (n = 5) bearing 200-mg LS174T tumors received 10 μCi of internalizing ^{64}Cu-DOTA-cBR96 or non-internalizing ^{64}Cu-DOTA-cT84.66. Tissues collected from 15 min-48 h post-injection were weighed and counted to calculate percent injected activity per organ (% IA/organ) and mouse tumor dosimetry from time-activity curves (TACs) (3). Alternatively, mice (n = 3) bearing 800-mg LS174T xenografts received RIT doses of 0.89 mCi of ^{64}Cu-DOTA-cBR96 or 0.71 mCi of ^{64}Cu-DOTA-cT84.66, to give normalized tumor absorbed doses. PET images were acquired on a Philips MOSAIC scanner, and CT imaging was performed on an ImTek microCAT II scanner. Each mouse was imaged from 3-48 h post-injection, and PET region of interest analyses were used to determine % IA/organ. CT imaging afforded 3-dimensional tumor volume measurements.

Conventional and PET/CT biodistributions of the ^{64}Cu-labelled mAbs are compared in Table 1. There were no significant differences ($p > 0.05$) in tumor uptake between the 2 mAbs at any time point in either study. The areas under the TACs were approximately twice as great for the PET/CT study. Because the tumors were approximately 4 times larger, absorbed doses (Table 1) calculated from PET/CT were approximately half those estimated by conventional methods. Correcting for injected activity, PET tumor doses for ^{64}Cu-DOTA-cBR96 and ^{64}Cu-DOTA-cT84.66 RIT were 4.31 and 4.56 Gy, respectively. These doses were within 95% agreement, despite individual variability, limitations of sacrificial experiments, and great disparity in tumor size between the 2 studies.

Mouse PET dosimetry offers great advantages for preclinical RIT using ^{64}Cu. For example, carefully controlled mouse RIT studies at normalized tumor absorbed doses can be performed. The results of such studies will be presented.

Acknowledgments: This research was funded by the University of Missouri College of Veterinary Medicine Committee on Research. The production of ^{64}Cu at Washington University is supported by NIH Grant CA86307 from the National Cancer Institute. We would like to thank Drs. Clay Siegall, Jack Shively, and Andrew Raubitschek for providing the mAbs used.

References:

1. Connett, J.M., *et al.*, *Proc. Nat. Acad. Sci. USA* **93:** 6814-6818 (1996).
2. Bryan, J.N., *et al.*, *Vet. Comp. Oncol.* **2:** 82-90 (2004).
3. Miller, W.H., *et al.*, *Trans. Am. Nucl. Soc.* **89:** 689-692 (2003).

Table 1. Tumor uptakes and absorbed doses for LS174T-bearing mice receiving ^{64}Cu-DOTA-cBR96 or ^{64}Cu-DOTA-cT84.66.

Time (h)	^{64}Cu-DOTA-cBR96 Tumor Uptake (% IA/organ, mean ± s.d.)	^{64}Cu-DOTA-cT84.66 Tumor Uptake (% IA/organ, mean ± s.d.)	^{64}Cu-DOTA-cBR96 Tumor Dose rad/mCi (mGy/MBq)	^{64}Cu-DOTA-cT84.66 Tumor Dose rad/mCi (mGy/MBq)
3[a]	4.43 ± 3.29	1.92 ± 0.71		
24	1.67 ± 0.56	1.78 ± 1.01		
48	0.14 ± 0.01	0.65 ± 0.23	1130 (305)	1410 (381)
3[b]	4.30 ± 3.83	12.1 ± 10.4		
24	3.35 ± 1.74	4.72 ± 1.94		
48	1.17 ± 0.49	1.47 ± 0.69	484 (131)	643 (174)

[a]Conventional. [b]PET/CT.

Keywords: Mouse PET/CT, Copper-64, Radioimmunotherapy

THE HUMAN NOREPINEPHRINE TRANSPORTER (hNET) IN COMBINATION WITH [^{11}C]m-HYDROXYEPHEDRINE ([^{11}C]mHED) AS REPORTER GENE/PROBE FOR GENE THERAPY

A.R. Buursma,[1] A.M.J. Beerens,[1] E.F.J. de Vries,[2] A. van Waarde,[1] M.G. Rots,[2] G.A.P. Hospers,[3] W. Vaalburg,[1] H.J. Haisma.[2]

[1]PET Center, University Medical Center Groningen, Groningen, Netherlands; [2]Therapeutic Gene Modulation, University of Groningen, Groningen, Netherlands; [3]Medical Oncology, University Medical Center Groningen, Groningen, Netherlands.

Objective: The herpes simplex virus thymidine kinase (HSVtk) gene has been studied extensively as a reporter gene for monitoring gene therapy. HSVtk, however, is not an ideal reporter gene. HSVtk could provoke an immune reaction in humans, since it is an exogenous gene. Moreover, imaging of HSVtk could be influenced by active transport of the tracer across the cell membrane, as the enzyme is located inside the cell. In search for a reporter gene that does not have these disadvantages, we investigated the potential of the human NET gene (hNET) in combination with the PET tracer [^{11}C]mHED.**Methods:** COS-7, A2780 and U373 cells were transiently transduced with various amounts of an adenoviral vector, containing the hNET gene and the enhanced green fluorescence protein (eGFP) gene in identical but separate expression cassettes (AdTrack-hNET). In this vector hNET acts as a reporter gene, whereas eGFP can be considered as a surrogate for a therapeutic gene. Two days after the application of the viral vector, eGFP expression was monitored by fluorescence measurement. Cellular [^{11}C]mHED uptake was determined by incubating the transduced cells with the tracer for 1 h in the presence or absence of the potent hNET antagonist desipramine (DMI; 6 μM). hNET protein levels in U373 cells were analyzed by dotblot and immunohistochemistry. In addition, [^{11}C]mHED biodistribution studies were performed in nude rats with two U373 tumor xenografts that were in-vivo transduced with either AdTrack-hNET or a control virus two days before. One hour after tracer injection, the tumors were dissected and weighed and radioactivity was measured. In random tumor sections, eGFP fluorescence was assessed.**Results:** In each of the transduced cell lines, [^{11}C]mHED uptake increased linearly with increasing viral titer and correlated well with viral titer ($r^2 \geq 0.95$, $P<0.05$). Cellular [^{11}C]mHED uptake could be reduced to baseline levels by DMI, indicating that tracer uptake was specifically mediated by hNET. At identical virus titers, [^{11}C]mHED uptake was 12 and 50 times higher in transfected U373 cells than in transfected COS-7 and A2780 cells, respectively. This phenomenon is most likely due to cell type-dependent transfection efficiencies. A good correlation between the amount of hNET protein and the [^{11}C]mHED uptake in U373 cells was observed ($r^2 = 0.99$; $P<0.0001$), indicating that the transduced hNET gene provides a functional enzyme and that [^{11}C]mHED uptake indeed reflects the magnitude of hNET expression. In all cell lines, eGFP fluorescence correlated well with the [^{11}C]mHED uptake ($r^2>0.96$; $P<0.005$), demonstrating the feasibility of hNET as a reporter gene for monitoring the expression of a therapeutic gene. In-vivo gene transfer was extremely low, as eGFP fluorescence could only be visualized in a single small patch of approximately 1 mm in diameter in 2 out of 24 series of tumor sections. Still, average [^{11}C]mHED uptake that was measured in the whole tumor was significantly higher ($p<0.05$) in AdTrack-hNET transduced tumors (0.125±0.015 %ID/g) than in tumors transduced with control virus (0.105±0.011 %ID/g).**Conclusion:** Taken together, these results demonstrate the potential of hNET in combination with [^{11}C]mHED as a reporter gene / probe system for monitoring gene transfer in gene therapy with PET.

Keywords: Gene Therapy, [^{11}C]mHED, Norepinephine Transporter

NUCLEAR IMAGING OF NANOPARTICLES IN XENOGRAFT TUMOR MODELS

Y.W. Cho,[1,2] S.A. Park,[1,3] M. Lee,[1] J.S. Park,[1,2] D.H. Son,[1,3] S.J. Oh,[2] D.H. Moon,[2] S.Y. Kim,[3] I.C. Kwon,[4] I.-S. Kim.[5]

[1]Asan Institute for Life Science, University of Ulsan College of Medicine, Seoul, Korea; [2]Department of Nuclear Medicine, Asan Medical Center, University of Ulsan College of Medicine, Seoul, Korea; [3]Department of Otolaryngology, Asan Medical Center, University of Ulsan College of Medicine, Seoul, Korea; [4]Biomedical Research Center, Korea Institute of Science and Technology, Seoul, Korea; [5]Department of Biochemistry, School of Medicine, Kyungpook National University, Daegu, Korea.

The enhanced permeability and retention (EPR) effect, which has been known as unique biological characteristics in rapid growing tumors, is now extensively used for passive targeting of many macromolecular drugs to tumors. In fact, the EPR concept has been a gold standard in polymeric drug delivery systems. Here we propose the change in modality from water-soluble macromolecular drugs to long-circulating polymeric self-assembled nanoparticles to realize the tumor-selectivity based on the EPR effect. We hypothesized that the particulate systems which have an appropriate size suited for the large open endothelial gaps in tumors and can stably circulate in the bloodstream, should actualize the passive tumor targeting by the EPR effect. Polymeric self-assembled nanoparticles were prepared from amphiphilic chitosan derivatives. The size of nanoparticles were varied from 150 to 500 nm in a mean diameter, which are aimed to be larger than an endothelial gap in normal tissues but smaller than a characteristic pore cut-off size in tumor tissues. FITC-labeled or ^{131}I-labeled nanoparticles were injected into the tail veins of tumor-bearing mice, and their body distribution was examined and visualized by gamma camera imaging. The polymeric self-assembled nanoparticles were sustained at a high level throughout 6 days, indicating their long systemic retention in blood circulation. The nanoparticles were gradually accumulated in tumors for 6 days. This highly selective tumoral accumulation of the nanoparticles should be mostly attributable to the optimized size for the open endothelial gaps in tumors and their long residence in blood circulation. Furthermore, the tumoral accumulation of the nanoparticles was visualized by nuclear imaging technology, which is the first one to clearly show the selective tumor-targeting by polymeric self-assembled nanoparticles.

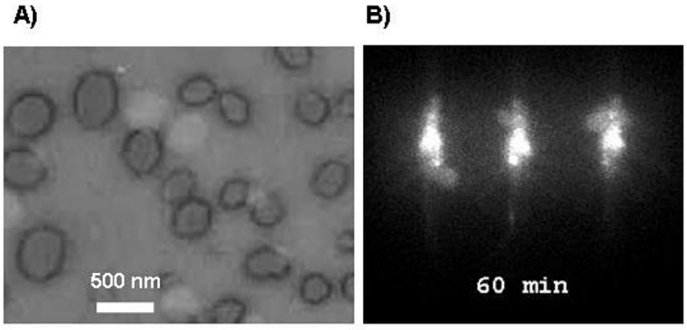

Figure 1. (A)TEM picture of nanoparticles and (B) gamma camera imaging of tumor-bearing mice

Keywords: Nanoparticles, Tumors, Nuclear Imaging

TUMOR PRETARGETING—FROM EMPIRICAL OPTIMIZATION TO MATHEMATICAL PREDICTION

G. Liu, S. Dou, J. He, X. Liu, M. Rusckowski, D.J. Hnatowich.
Division of Nuclear Medicine, University of Massachusetts Medical School, Worcester, MA, United States.

Compared to "conventional" tumor targeting with radiolabeled antitumor antibodies, tumor pretargeting using unlabeled antitumor antibodies as the first injectate to be followed by a radiolabeled effector may be an improved method of delivering radioactivity to tumor. We have shown that pretargeting with phosphodiamidate morpholios (MORF) is capable of providing superior tumor to normal tissue radioactivity ratios more rapidly than is possible using radiolabeled antibodies. However pretargeting with its multiple injections is more complicated and requires more effort in optimization. **OBJECTIVE:** To develop a mathematical description capable of predicting the accumulations in tumor of the MN14 antiCEA antibody (conjugated with MORF) and the ^{99m}Tc radiolabel (attached to the complementary cMORF). **METHODS**: Using nude mice bearing LS174T tumors in one thigh, the pharmacokinetics of ^{111}In-MN14 antibody, assumed to be identical to the antibody-MORF, and the pharmacokinetics of ^{99m}Tc labeled cMORF were both determined. Thereafter, a series of pretargeting studies were performed to establish organ accumulations of ^{99m}Tc-cMORF administered at various dosages. Accessibility of antibody-MORF to labeled cMORF was determined from the ^{111}In-antibody values and the accumulations of ^{99m}Tc labeled cMORF. Mathematical descriptions of organ accumulation as a function of antibody-MORF expression and the dosage of labeled cMORF were then developed based on the pharmacokinetics of both injectates. Finally, a pretargeting study was performed to test the agreement between the experimental and the calculated values. **RESULTS:** Tumor CEA antigen was not saturated by the antiCEA MN14 antibody even at the highest dosage investigated (100 μg per mouse). Furthermore, the tumor level of antibody was constant at least for 3 days post antibody administration while levels in normal organs gradually decreased. The accessibility to ^{99m}Tc-cMORF to the antibody-MORF was quantitative in blood and tumor and less so in other organs. Before tumor saturation with labeled cMORF, the tumor accumulation of labeled cMORF was determined by the efficiency of its delivery to tumor, a quantity characteristic of the labeled cMORF and the tumor blood supply. After tumor saturation with labeled cMORF, tumor accumulation of ^{99m}Tc-cMORF was quantitatively related to the antibody-MORF expression. Kidney accumulations were independent of the antibody and dependent only on labeled cMORF itself. Antibody-MORF in all other organs was easily saturated and therefore also quantitatively related to the antibody-MORF expression. Mathematical prediction and the experimental data were in gratifying agreement, suggesting that the mathematical description of the pretargeting process was reliable. **CONCLUSION:** Based on the mathematical description of the pharmacokinetics of MN14-MORF and labeled cMORF as well as their quantitative relationships, pretargeting results can be predicted for a set of given pretargeting variables, demonstrating that the pretargeting process is understood.

Keywords: Tumor Pretargeting, Prediction, Radioimmuno-Detection and -Therapy